

# Simple and Rapid Adhesion of Commodity Polymer Substrates under Ambient Conditions Using Complexed Alkylboranes

Olivia R. Wilson, Dominick J. Borrelli, and Andrew J. D. Magenau\*

Cite This: *ACS Omega* 2022, 7, 28636–28645

Read Online

ACCESS |

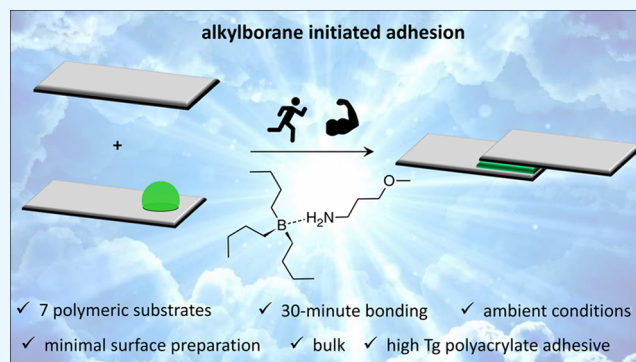
Metrics &amp; More

Article Recommendations

Supporting Information

**ABSTRACT:** Adhesives are ubiquitous in manufacturing spanning nearly all sectors from healthcare and photovoltaics to aerospace and electronics. Yet many commercial polymers remain challenging to adhere, necessitating either pretreatment, mechanical fastening, or adhesive processes that involve specialized equipment, high temperature/vacuum, and long cure times. Thus, rapid-cure adhesives for polymers that can set under ambient conditions using simple procedures are desirable because they offer cost savings, faster production, and greater design freedom to producers. Herein, we report a powerful adhesive platform that bonds a wide scope of commodity polymers via (hydrogen) atom transfer and free-radical (graft) polymerization initiated with a trialkylborane–ligand complex and isocyanate decomplexing agent.

The developed adhesive formulation is air-stable, bulk, and operates in air at room temperature using a high-glass-transition temperature polyacrylate, i.e., poly(isobornyl acrylate). The alkylborane-initiated bonding process is rapid (~30 min), requires minimal surface preparation (cleaning and mild roughening), and successfully bonds seven diverse substrates including polytetrafluoroethylene, polyethylene, polypropylene, polycarbonate, nylon, polymethylmethacrylate, and polyvinylchloride. This contribution uniquely investigates the process–property relationships for the adhesive formulation, lap-shear performance, mechanism of failure, and a reactive additive for enhancing the adhesive's glass-transition temperature to ~120 °C (polyhedral oligomeric silsesquioxane or POSS) to widen its operation temperature. We envision that the reported alkylborane-initiated adhesion platform could hold promise in the automotive, aerospace, and marine sectors as means for rapid manufacturing and structural adhesion.



## 1. INTRODUCTION

Adhesives are a central aspect of numerous manufacturing and assembly processes, spanning healthcare, photovoltaics, automotive, and aerospace sectors.<sup>1</sup> Despite their vast implementation, many polymeric substrates of commercial relevance remain notoriously difficult to adhere,<sup>2</sup> especially with the most widely produced polyolefins like polyethylene and polypropylene.<sup>3</sup> Commonly, when attempting to adhere such polymer substrates, poor adhesion and hence mechanical properties are obtained, mandating the use of expensive pretreatment (e.g., corona, flame, plasma, acid treatments)<sup>2,3</sup> or post-adhesion reinforcement by mechanical fastening.<sup>4</sup> Compounding the prior problem, even when adhesion is possible, the process of adhesion can be inefficient and complex involving specialized equipment and/or conditions consisting of high temperatures, long cure times, and vacuum.<sup>2</sup> Today, epoxy adhesives are one of the most commonly used structural adhesives for bonding in the automotive, aerospace, and electronic sectors;<sup>4</sup> however, these adhesives commonly require multiple hours to bond and staged curing schedules involving multiple/elevated temperatures or reduced pressures.<sup>5–7</sup> Hence, rapid-cure adhesives for polymeric substrates

that can set under ambient conditions and use simple processes are desirable, thus enabling cost savings, faster production, and greater design freedom to producers.

Herein, we seek to develop a simple, versatile, and rapid bonding system composed of a moderately high operation temperature adhesive with minimal surface pretreatment. We envisioned that complexed alkylboranes, a subject our group and others, have recently pursued for various purposes,<sup>8–14</sup> could enable such an adhesion process because they offer rapid rates, room-temperature radical reactions, and safe handling under atmospheric conditions. While alkylborane adhesion of polymeric substrates has been disclosed via free-radical polymerization, primarily in expired patents<sup>15–20</sup> and briefly in the literature using methacrylate (co)polymerizations,<sup>21–23</sup>

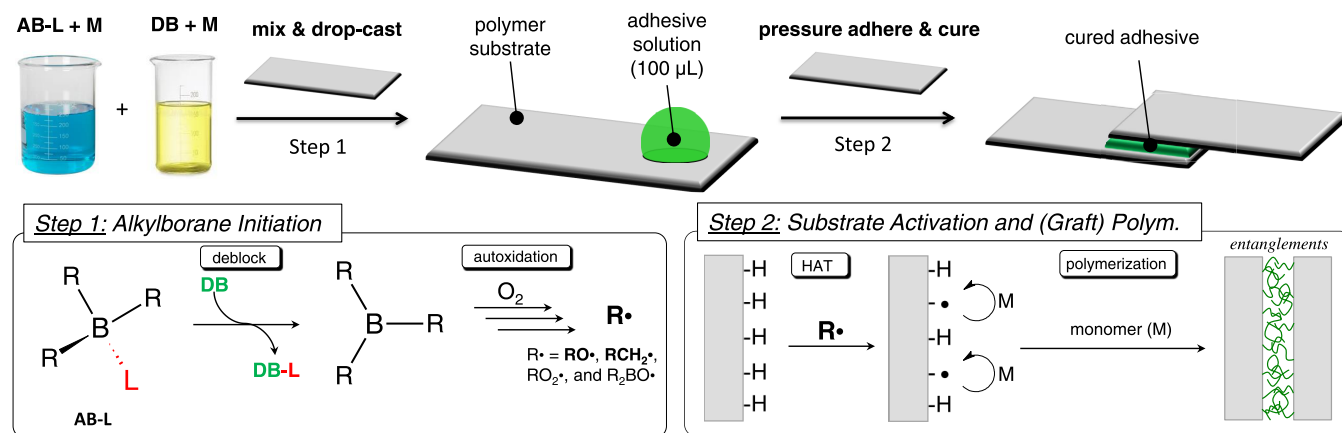
Received: June 15, 2022

Accepted: July 26, 2022

Published: August 2, 2022



## Scheme 1. Reaction Mechanism and Adhesion Process via Complexed Alkylboranes under Ambient Conditions



to our knowledge nothing has been reported on solely acrylate-based alkylborane adhesives. In these literature reports, methyl methacrylate was polymerized alone or with butyl acrylate on polypropylene or polyethylene. Here, we explore a new acrylate-based adhesive with a relatively high-glass-transition temperature that exhibits rapid/ambient bonding with seven commodity polymer substrates. An acrylate-based adhesive was an important design criterion because the monomer should provide favorable kinetics needed for a rapid and high-yielding adhesive under ambient conditions. In this contribution, we uniquely take an in-depth look into the process–property relationships for the adhesive formulation, lap-shear performance, mechanism of failure, and substrate scope and explore a reactive additive for further enhancement of the adhesive’s thermal properties and operating temperature.

Toward our goal, we developed a two-step, reactive adhesion process for commodity polymer substrates using an alkylborane–ligand complex (AB–L). In the first step, a solution of AB–L in the monomer (M) is combined with a second solution of a deblocker (DB) in the monomer that is then cast onto a polymeric substrate, as shown in Scheme 1 (Step 1). During this step, the complexed alkylboranes are deblocked, generating uncomplexed trialkylboranes, which autoxidize at diffusion-controlled reaction rates<sup>24</sup> and in turn produce several types of radicals (alkoxy, alkyl, peroxy, and boryl radicals).<sup>25</sup> In the second step, while pressing the adhesive between two substrates, the generated radicals simultaneously initiate free-radical polymerization and graft polymerization from the substrate (Scheme 1, Step 2). Unlike other radical processes, alkylborane initiation tolerates atmospheric conditions and can avert O<sub>2</sub> inhibition because it consumes O<sub>2</sub> during radical generation.<sup>9,26,27</sup> Moreover, in the second step, interfacial bonds and entanglements are formed between the adhesive and the substrate primarily through hydrogen atom transfer (HAT), which introduces radicals onto the substrate’s polymeric backbone that initiate graft polymerization.<sup>25,28</sup> Alkoxy radicals are well-known to participate in HAT reactions<sup>29</sup> and are one of the major radical products generated from the autoxidation of alkylboranes.

## 2. EXPERIMENTAL SECTION

**2.1. Reagents and Materials.** All monomers were used as received including isobornyl acrylate (IBOA, Sigma-Aldrich), isobornyl methacrylate (VWR), and styrene (Acros Organics). The AB–L complex, tri-*n*-butylborane 3-methoxypropylamine,

was donated from Callory LLC (Pittsburgh, PA) and stored in a glovebox. All other reagents, including isophorone diisocyanate (IPDI, 98%, Sigma-Aldrich), methacrylic acid (TCI Chemicals), polyhedral oligomeric silsesquioxane with eight acrylopropyl groups (90%, Hybrid Plastics), and Super P carbon black (99+%, Alfa Aesar), were used as received. All polymer substrates were ordered from McMaster-Carr and cut into 10.2 × 2.5 × 0.3 cm (4 × 1 × 1/8 inch) specimens from original bars of 38 × 1 × 1/8 inch. The polymer substrates include polypropylene (part number: 8782K11), polycarbonate (part number: 1749K119), high-density polyethylene (part number: 8671K11), polytetrafluoroethylene (part number: 8735K12), nylon 66 (part number: 8733K11), polyvinylchloride (part number: 8740K11), and polymethylmethacrylate (part number: 1227T119).

**2.2. Characterization.** **2.2.1. Single Lap-shear.** Single lap-shear tensile tests were performed on a servohydraulic Instron using either a 1 or 25-kilonewton load cell. All tensile tests were carried out at room temperature under a crosshead speed of 1.27 mm/min (0.05 in/min) in accordance with ASTM D1002-10.<sup>30</sup> A pair of self-aligning grips were used to hold the outer 2.25 inch of each end of the single lap-shear joint. Mechanical properties including modulus, stress at break, strain at break, and toughness were calculated from generated stress–strain data. The elastic modulus was quantified as the slope of the stress–strain curve up to 0.2% strain. The stress and strain at break were reported at the point of failure for the alkylborane adhesive. Toughness was calculated as the area under the stress–strain curve until the point of failure using OriginLab software. All mechanical properties were reported as the mean values of at least three replicates and the error as one standard deviation about the mean.

**2.2.2. Nuclear Magnetic Resonance (NMR).** Proton NMR was used to calculate all monomer conversions from vial polymerizations. NMR spectra were obtained using a Varian Unity Inova 500 MHz spectrometer at room temperature with CDCl<sub>3</sub> as the deuterated solvent. All spectra were recorded using 64 scans with a relaxation delay time of 1 s. All chemical shifts were referenced to chloroform.

**2.2.3. Differential Scanning Calorimetry (DSC).** DSC was used to calculate the glass-transition temperature of the adhesive formulations synthesized from vial polymerizations. Thermograms were recorded using a heat/cool/heat procedure with a ramp rate of 10 °C/min. The glass-transition temperature was identified at the inflection point from the

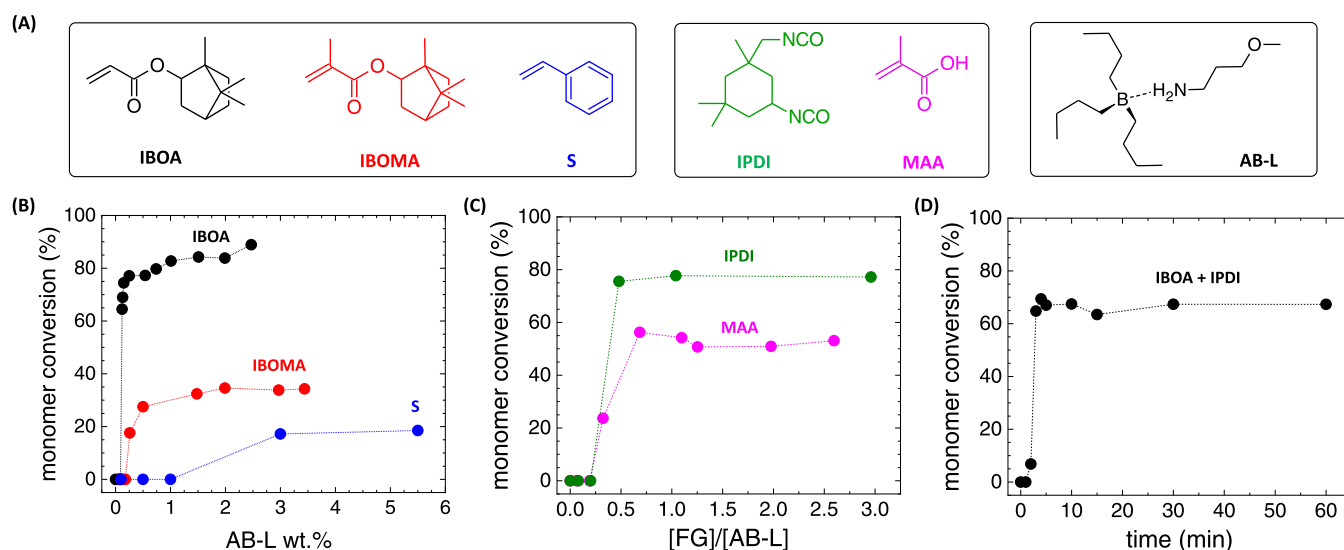


**Figure 1.** (A) Chemical structures of monomers, deblockers, and initiators used in optimizing the adhesive formulation. (B) Evaluation of three monomer classes using AB–L initiation. Conditions: bulk polymerization with IPDI deblockers and  $[\text{NCO}]/[\text{AB–L}] \approx 1.25/1$  for 24 h. (C) Evaluation of the deblocking functional group (FG) and concentration. Conditions: bulk polymerization with  $[\text{AB–L}] \approx 1$  wt % for 24 h. (D) Kinetics of IBOA polymerization. Conditions: bulk polymerization with IPDI deblockers,  $[\text{AB–L}] \approx 1$  wt %, and  $[\text{NCO}]/[\text{AB–L}] \approx 1.25/1$  for 24 h.

second heating cycle using Universal V4.5A TA Instrument software.

**2.2.4. Keyence VK-3000 Laser Profilometer.** The laser profilometer was used as a noncontact three-dimensional (3D) surface profiler to perform a high-resolution thickness analysis of the adhesive film and failure mechanism. Bond line thicknesses were conducted by averaging six measurements of the height change from the neat substrate to areas where the adhesive resided after failure. Failure analysis images were recorded from the same area on complimentary substrates of a single lap-shear joint after failure.

**2.3. Synthetic Procedures. 2.3.1. Alkylborane-Initiated Free-Radical Polymerization.** A representative alkylborane-initiated free-radical polymerization, formulated to have a  $[\text{AB–L}] \approx 1$  wt % and a molar ratio of  $[\text{NCO}]/[\text{AB–L}] \approx 1.25/1$ , was conducted as follows. The AB–L complex was removed from the glovebox and used within 3 h. Under ambient conditions, two 20 mL scintillation vials were used to prepare two stock solutions referred to as vials A and B. In vial A, 0.042 g of AB–L was added to 2.00 g of IBOA. In vial B, 0.022 g of IPDI was added to 2.00 g of IBOA. Each stock solution was separately vortexed for 15 min to ensure homogeneity. To commence polymerization, equal masses ( $\sim 2.00$  g) of vials A and B were combined in a new 20 mL scintillation vial and hand-mixed for 15 s. The scintillation vial was then left to polymerize without further interruption for 24 h. NMR was conducted after 24 h of polymerization and monomer conversion was quantified using the equation shown in Figures S1–S3.

**2.3.2. Substrate Preparation.** Polymer substrates were ordered from McMaster-Car and cut using a band saw into specimens of dimensions  $10.16 \times 2.54 \times 0.318$  cm ( $4 \times 1 \times 1/8$  inch), which were then assembled and bonded in a lap-shear configuration using a  $2.54 \times 2.54$  cm overlap area. Prior to adhering the substrates into single lap-shear joints, the substrates were first wiped with acetone. The wiped substrates were then sanded with an 80-grit sandpaper using three passes (forward–back–forward) in each orientation ( $-45/90/45^\circ$ )

to provide a consistent surface roughening. Following sanding, the surfaces were deburred thoroughly with a tack cloth to remove loose debris. Next, the substrates were cleaned with a final acetone wash. These steps were followed for each type of substrate, except for polycarbonate and polymethylmethacrylate, which were wiped with hexanes instead of acetone.

**2.3.3. Lap-shear Joint Preparation.** Lap-shear specimens were synthesized in sets of five to ensure that average mechanical values could be calculated. To do so, a lap-shear jig was fabricated to facilitate consistent preparation of the lap-shear specimens. After the substrates were prepped using the method described in Section 3.2., the lap-shear jig was sprayed with a nonstick Teflon spray. Once the spray dried, the overlap region on the fixture was covered with an aluminum foil to prevent the samples from sticking to the jig. The substrates were then placed into the jig and adhered using 100  $\mu\text{L}$  of the reaction mixture (i.e., the adhesive), which fully covered the overlap area with minimal flash. Finally, a one-kilogram weight was immediately placed on top of the overlap region for 1 h, unless otherwise stated.

**2.3.4. Synthesis of the Poly(isobornyl acrylate) Adhesive and Lap-shear Joints.** All formulations used for testing were performed in bulk (no solvent). The AB–L complex was removed from the glovebox and used within 3 h. A representative alkylborane-initiated adhesion experiment, formulated to have a  $[\text{AB–L}] \approx 1$  wt % and a molar ratio of  $[\text{NCO}]/[\text{AB–L}] \approx 1.25/1$ , was conducted as follows. Under ambient conditions, two 20 mL scintillation vials were used to prepare two stock solutions referred to as vials A and B. In vial A, 0.044 g of AB–L was added to 2.00 g of IBOA. In vial B, 0.022 g of IPDI (equivalent to 0.20 mmol NCO) was added to 2.00 g of IBOA. Each stock solution was separately vortexed for 15 min to ensure homogeneity. To commence polymerization, equal masses ( $\sim 2.00$  g) of vials A and B were combined in a new 20 mL scintillation vial and hand-mixed for 15 s. Afterward, 100  $\mu\text{L}$  of the reaction mixture was immediately transferred to the middle of the exposed overlap region of the substrates held in the lap-shear jig. Immediately

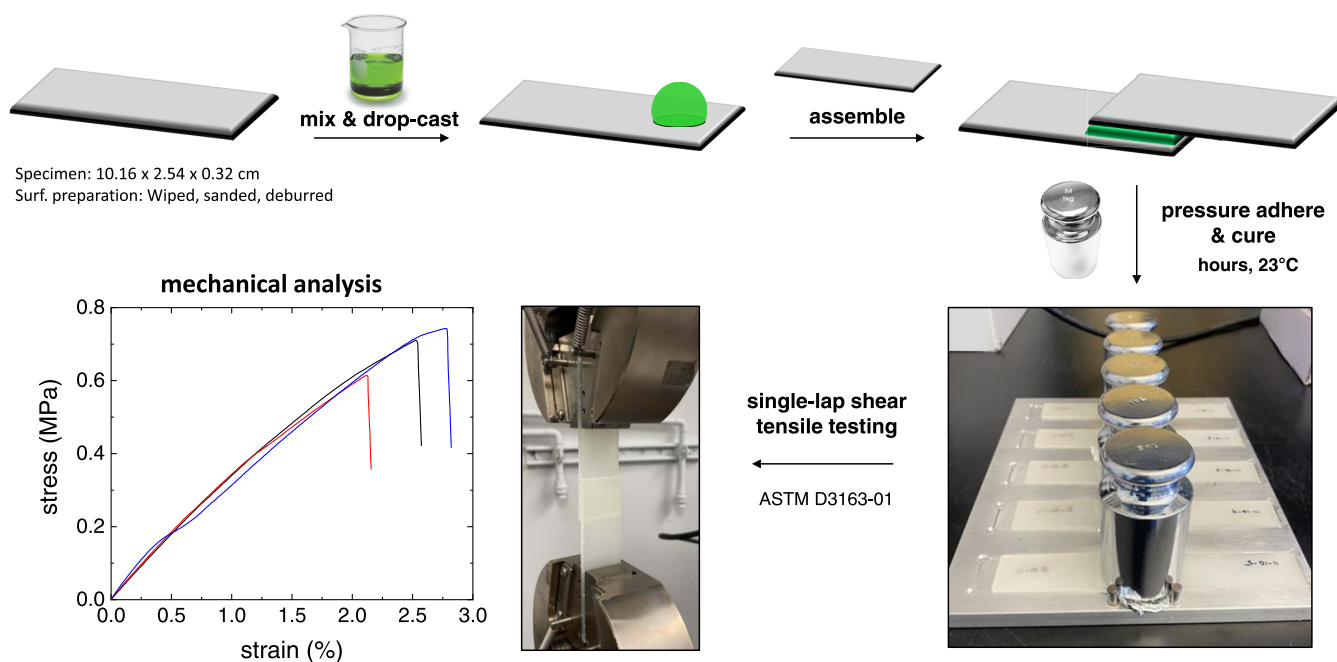


**Figure 2.** Schematic of the adhesion process, mechanical testing, and analysis of lap-shear specimens fabricated using alkylborane adhesion.

thereafter, the second substrate was placed on top of the adhesive and first substrate so that there was a 1-inch overlap. Finally, a one-kilogram weight was immediately placed on top of the overlap for 1 h, unless otherwise stated. The same procedure was utilized for the incorporation of carbon black or POSS by adding them to vial A. We note that the mol. % POSS was calculated as the percentage of moles from POSS over the summation of the moles from AB-L, POSS, IPDI, and IBOA.

### 3. RESULTS AND DISCUSSION

**3.1. Determining the Adhesive Formulation: Monomer, Deblocator, and Kinetics.** Before carrying out lap-shear tests to evaluate performance, we first sought to optimize our formulation for the monomer/deblocator and to gain a sense of the polymerization kinetics. Three classes of monomers (acrylate, methacrylate, styrenic) and two classes of deblockers (isocyanate, carboxylic acid) were explored to optimize the system for a maximum monomer conversion. As shown in Figure 1A, we selected isobornyl acrylate (IBOA), isobornyl methacrylate (IBOMA), and styrene (S) as the monomers and isophorone diisocyanate (IPDI) and methacrylic acid (MAA) as the deblockers. The monomers were selected because of their inertness toward the AB-L complexes, hydrophobicity, low-vapor pressure, and their polymers' relatively high-glass-transition temperatures ( $T_g \geq 90$  °C).<sup>31</sup> System performance was evaluated via bulk polymerizations under fully ambient conditions by combining an initial solution of deblockers in monomers with a second solution of AB-L in monomers. After briefly mixing, the polymerization mixtures were allowed to react for 24 h before the conversion was determined by NMR (see Figures S1–S3).

Our experimentation revealed that acrylates performed the best, providing the highest conversion of monomer with the least amount of AB-L initiator under ambient conditions (Figure 1B). For example, at 0.5 wt % of AB-L, IBOA achieved a monomer conversion of ~78%, whereas IBOMA reached only ~28% and styrene ceased to exhibit polymerization. In addition to monomer conversion, the acrylate

system required the least amount of AB-L to initiate polymerization compared to the methacrylate and styrenic monomers. The onset of polymerization for IBOA was only ~0.12 wt % of AB-L, whereas IBOMA required at least ~0.26 wt % and styrene required excessive amounts of AB-L (> 1 wt %) for any polymerization to occur. These conversion trends can be rationalized by the propagation rate coefficients of the monomer classes at 30 °C (acrylate  $\approx 1\text{--}3\text{E}4$ , methacrylate  $\approx 4\text{--}9\text{E}2$ , styrene  $\approx 1\text{E}2$   $\text{M}^{-1} \text{s}^{-1}$ ) with larger rate coefficients favoring higher polymerization rates and conversions under similar conditions.<sup>32</sup> Hence, moving forward, we down-selected our monomers to IBOA and elected to employ a [AB-L]  $\approx 1$  wt % to be safely above the onset of polymerization and to ensure moderate-to-high levels of conversion.

To investigate deblocker type and its concentration, a series of polymerizations were conducted with either IPDI or MAA deblockers under a range of concentrations. These experiments are shown in Figure 1C and the concentration of deblockers is reported as the molar ratio of deblocking functional groups to initiators or  $[\text{FG}]/[\text{AB-L}]$ . Our experiments reveal that neither deblocker could induce any significant amount of polymerization until the  $[\text{FG}]/[\text{AB-L}]$  ratio exceeded 0.2, after which the conversion was found to plateau around 75–80% for IPDI and 50–55% for MAA. These results align with our previous experimentation showing that isocyanates are more efficient deblockers than weak acids when employed at low concentrations.<sup>9</sup> Moreover, the methacrylate functionality on MAA likely contributed to the observed reduction in conversion compared to the IPDI system. Finally, to gain a sense of the kinetics, we selected IPDI as the deblocker because of its higher conversions and employed it at a molar ratio of  $[\text{NCO}]/[\text{AB-L}] \approx 1.25$  going forward. Kinetic studies showed that the polymerization of IBOA was very rapid, achieving a maximum conversion of monomers in less than 5 min (Figure 1D), accompanied by a large exotherm to ~100 °C in a few minutes. This outcome was not unexpected considering the polymerizations were bulk and with an acrylic

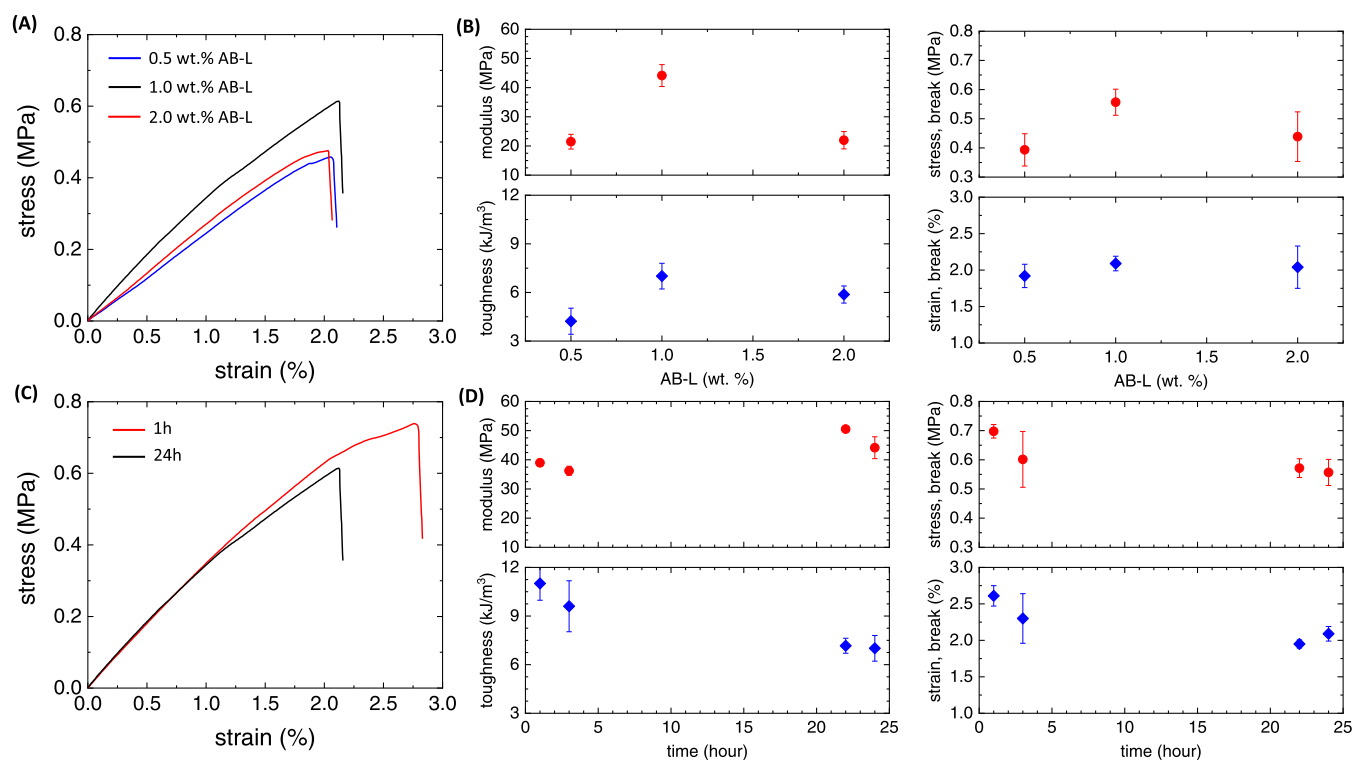


**Figure 3.** (A, B) Impact of AB-L concentration on the adhesive performance using PP substrates. Adhesive system: bulk IBOA, [NCO]/[AB-L]  $\approx$  1.25/1, weight press time = 1 h, and cure time = 24 h. (C–D) Impact of time between synthesis and testing on adhesive performance using PP substrates. Adhesive system: bulk IBOA, [AB-L]  $\approx$  1 wt %. [NCO]/[AB-L]  $\approx$  1.25/1, weight press time = 1 h, and cure time = 1, 3, 22, and 24 h.

monomer. We and others have observed rapid polymerization rates when using acrylates and acrylamides in concentrated polymerizations.<sup>10,27,33</sup> From these experiments, we identified an optimal adhesive formulation that maximized monomer conversion within a short timeframe, helping to facilitate a rapid/ambient condition adhesion technology with a high-glass-transition temperature poly(acrylate).

**3.2. Understanding the Impact of Initiator Concentration and Bonding Time on Performance.** After optimizing our adhesive formulation for monomer conversion, we devised a simple bonding procedure to adhere polymeric substrates under ambient conditions. As illustrated in Figure 2, assembled lap-shear specimens were fabricated by placing 100  $\mu$ L of our optimized adhesive onto an adherend and then compressing the adhesive between a second adherend. Once assembled, a one-kilogram weight was placed on top of the adhesive joint for an hour, and the specimen was then allowed to cure for an allotted time. The reported bonding process conformed to ASTM D3136<sup>30</sup> and was purposefully designed to exclude complex surface treatments (corona discharge, plasma, flame) or laborious curing profiles with staged heating/vacuum that would necessitate equipment. All of the lap-shear specimens were assembled in a jig to ensure consistent alignment between adherends, and the mechanical properties are reported as a mean from at least three replicates. As an initial control, adhesions of polypropylene (PP) substrates with AB-L and DB alone (no monomer) were found to be incapable of providing a strong bond and easily fractured during loading into the tensile tester, underscoring the necessity of monomers.

Our initial lap-shear experiments were designed to understand the impact of [AB-L] and bonding time on performance. First, we studied three AB-L concentrations with

representative stress–strain curves for each concentration shown in Figure 3A. Lap-shear experiments revealed that 1 wt % AB-L provided the best adhesive performance, exhibiting an improved toughness, stemming from a twofold enhancement in the modulus and an increased stress at break (see Figure 3B), compared to formulations with half or double the initiator. Strain at break values were largely unaffected under our experimental conditions. We speculate that the reduced performance of the adhesive at lower AB-L concentrations is a result of a reduced grafting density and monomer conversion, which would reduce polymer entanglements and plasticize the adhesive. Conversely, the high initiator concentration also experienced a poorer performance, which is attributed to a very rapid polymerization rate that provided insufficient time to apply the adhesive and assemble the lap-shear specimen before vitrification, thus preventing an intimate adherend–adhesive interface and alkoxy radical generation on the substrate’s surface for graft polymerization. These experiments highlight the importance of optimizing the AB-L concentration for performance and the delicate balance, which exists between maximizing the adhesive chemistry (HAT and grafting) but not at the expense of an overly diminished working time to apply the adhesive. To gain some insight into the contribution of the adhesive chemistry, we conducted an adhesion control experiment without any surface roughening. Impressively, even if weaker, the PP adherends were successfully bonded (Figure S5). On average, a twofold reduction in the modulus, stress at break, and strain at break were observed and a fivefold decrease in toughness. This result is not unexpected since adhesives applied as fluids provide stronger bonds when using roughened substrates since the true surface area is greater than its geometrical area.<sup>34</sup> Importantly though, this result underscores that the reaction and chemistry

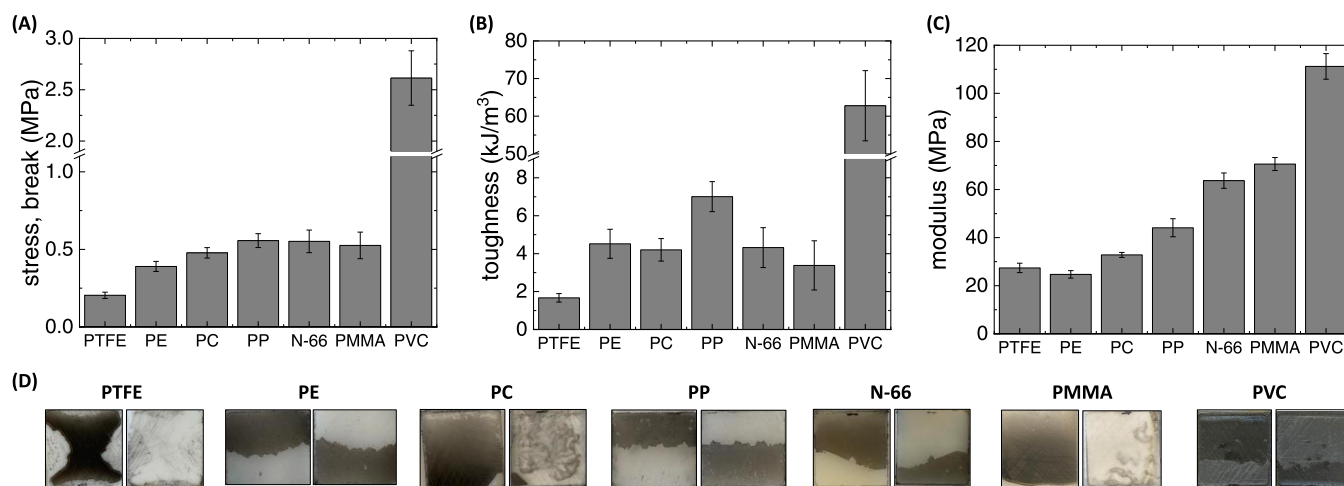


**Figure 4.** Adhesive performance and failure of seven commodity polymer substrates via alkylborane-initiated adhesion. (A) Stress at break values. (B) Toughness values. (C) Modulus values. Adhesive system: bulk IBOA,  $[AB-L] \approx 1$  wt %,  $[NCO]/[AB-L] \approx 1.25/1$ , weight press time = 1 h, and cure time = 24 h. (D) Images of failure surfaces after lap-shear tensile testing. Carbon black was added to the adhesive for contrast.

(HAT, surface grafting, polymerization, entanglements, etc.) play a contributing role to the adhesive's mechanical performance and that mechanical integration from roughening is not the only factor.

Of central importance to our research was understanding the bonding time because of its implications in enabling rapid manufacturing and adhesion. Thus, we prepared a series of lap-shear specimens with an identical adhesive formulation and tested them over a range of cure times, i.e., from the time of assembly to the time of lap-shear testing. Overall, experimentation revealed that regardless of the cure time, adhesion between PP adherends was successful and that strong adhesive bonds formed rapidly. Representative stress–strain curves at short and long cure times are shown in Figure 3C. Lap-shear specimens prepared over the course of 24 h experienced some embrittlement evidenced by slightly higher moduli and reduced toughness values, the latter of which stems from lowered stress and strain at break values (Figure 3D). We speculate that longer cure times allow for a continued reaction, which would reduce any plasticization by residual monomers and likely cause further contraction of the adhesive and more internal stresses. Regardless, to further explore the limits of cure time, we conducted one last experiment having a 30 min weight press and cure time, which successfully bonded the PP adherends at a comparable performance level (Figure S4). It is important to note that this result is not directly comparable to those reported in Figure 3C,D due to the differences in the weight press time (30 vs. 60 min). Collectively, however, these results demonstrate that the alkylborane adhesion system can be used as a powerful means for bonding polymeric substrates within minutes.

**3.3. Evaluating Substrate Scope, Performance, and Failure.** Encouraged by the successful bonding of PP, we investigated the breadth of commodity polymer substrates, which could be adhered using alkylborane-initiated adhesion. We rationalized that adhesion should be widely applicable to many polymer substrates since the alkylborane adhesion mechanism is generic, operating through an atom transfer mechanism involving radicals. For instance, in the case of PP, alkoxy radicals generated from the autoxidation of AB-L are known to participate in hydrogen atom transfer from the 3° carbons in the polymer's backbone.<sup>28,35</sup> Thus, based on this

generality, we selected and attempted to adhere six additional commodity substrates (Figure 4) including polytetrafluoroethylene (PTFE), polyethylene (PE), polycarbonate (PC), nylon 66 (N-66), poly(methyl methacrylate) (PMMA), and polyvinylchloride (PVC). In each case, we utilized the same adhesive formulation of 1 wt % AB-L, a ratio of  $[NCO]/[AB-L] \approx 1.25/1.0$ , and a cure time of 24 h established from our previous experiments. Strikingly, the alkylborane adhesion system was found to bond all of the polymer substrates. According to stress at break values (Figure 4A), PVC produced the strongest bond at  $\sim 2.6$  MPa and PTFE produced the weakest bond at  $\sim 0.2$  MPa, whereas the remaining four substrates had an intermediate level of performance between  $\sim 0.4$  and  $0.6$  MPa. Strains at break values were relatively independent of the substrate type, all residing between  $\sim 1$  and  $2\%$  strain with exception of PVC, which had a value of  $\sim 4\%$  (Figure S7).

To gain molecular-level insights into performance, we determined the toughness of each adhesive joint (Figure 4B), which is known to reflect the number of entanglements at the interface.<sup>36</sup> We speculated when using AB-L adhesion, the number of entanglements should be, in part, driven by the degree of grafting from the substrate and its dependence on the constituent bond dissociation energies within each polymer's backbone. Taking this into account, PVC was found to have the largest toughness, indicating that the adhesive generates the most entanglements with this substrate, likely stemming from an increased grafting density and reduced bond dissociation energy of the backbone C–Cl bonds ( $\approx 85$  kcal/mol).<sup>37</sup> In the case of PVC, carbon-centered radicals are also known to readily abstract chlorine and thus expected to contribute to an increased amount of grafting.<sup>38</sup> In contrast, PTFE had the lowest toughness value, suggesting a low degree of entanglements/grafting, a consequence of the strong C–F bonds (C–F  $\approx 127$  kcal/mol),<sup>37</sup> which are unlikely to participate in atom transfer reactions. The remaining substrates all had backbone C–H bonds with intermediate levels of strength of at least  $95$ – $99$  kcal/mol,<sup>37,39</sup> yielding toughness values of  $3.5$ – $4.5$  kJ/m<sup>3</sup>. The tertiary C–H bond of PP, at the bottom of the range ( $\sim 95$  kcal/mol), may also explain why PP had a slightly larger toughness of  $7$  kJ/m<sup>3</sup> compared to the rest of the group.

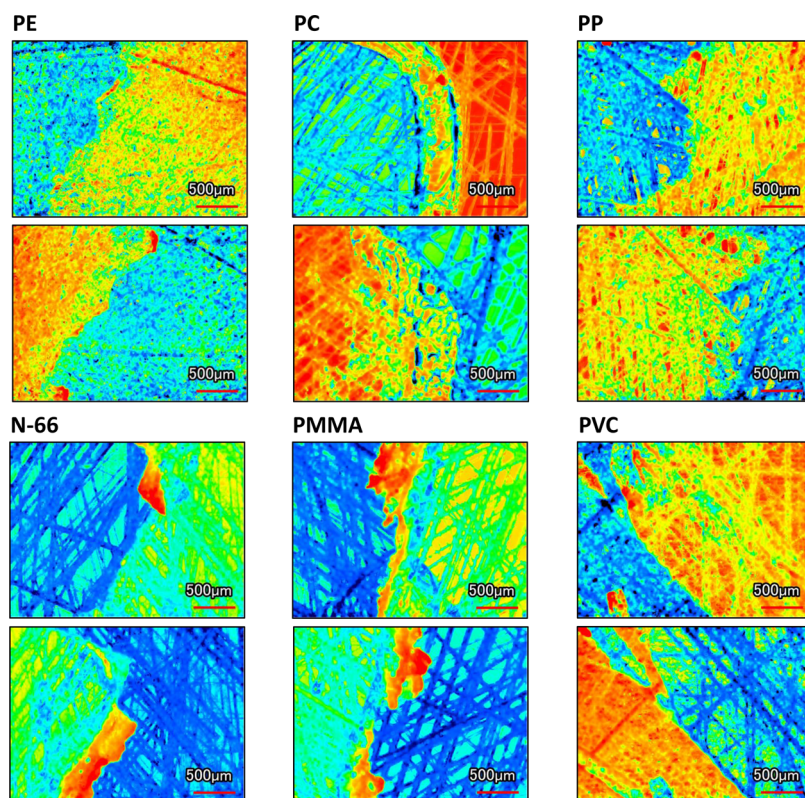


**Figure 5.** Top-down laser profilometer images of fracture surfaces in the overlap region of PE, PC, PP, N-66, PMMA, and PVC. Images were taken from the same area on complimentary substrates of a single lap-shear joint. Red regions correspond to larger heights, whereas blue regions correspond to lower heights.

In addition to the toughness, the lap-shear modulus was also evaluated, revealing a wide range of values with more nuanced levels of performance (Figure 4C). A glassy polymer's modulus is known to be related to the strength of interactions between polymer chains.<sup>40–42</sup> Therefore, since all of the substrates and pIBOA have glass-transition temperatures well-above room temperature,<sup>43</sup> we reasoned that the differences in moduli are a manifestation of the degree of favorable interactions at the interface between pIBOA and the adherend. In general, less-polar/fluorinated substrates exhibited lower moduli likely from poorer interactions with pIBOA (i.e., PTFE, PE, PC, and PP  $\leq$  45 MPa), whereas relatively more-polar substrates, closer to pIBOA, displayed enhanced moduli (i.e., Nylon, PMMA, PVC  $\geq$  45 MPa).

After performance evaluations, we attempted to understand the failure mechanism of the adhesive joint. Initial efforts were unsuccessful because the adhesive was clear, making it difficult to observe on the surface. Therefore, to improve contrast, a series of lap-shear specimens were generated with a small amount of carbon black in the adhesive formulation ( $\sim$ 0.15 wt %). Control experiments revealed that this low amount of carbon black had a negligible impact on adhesive performance (see Figure S8) and its ability to polymerize IBOA, i.e., conversion of  $\sim$ 79% with and  $\sim$ 83% without carbon black. Upon inspection of the failed surfaces at any given location within a pair (Figure 4D), the pIBOA adhesive was found almost exclusively on one side or the other, indicating an adhesive failure mode for all of the substrates. The light black areas in the right images of PC and PMMA are adhesive flash on the outside of the lap-shear joint and external to the overlap region (i.e., not adhesive materials between the adherends),

which can only be seen because the substrates are transparent. Visual inspection of PE, PP, N-66, and PVC revealed that the adhesive crack front started at each end of the overlap until meeting near the center of the joint when the catastrophic failure occurred. In the case of PTFE, the adhesive was only located in a smaller localized area of the overlap because of poor wetting and an inability to fully spread over the whole joint. To further confirm the failure mode on samples without carbon black, we employed laser profilometry, which allowed us to produce topological maps of complimentary areas from the two substrates that make up a single lap-shear joint (Figure 5). The images illustrate the average height of the neat substrate surface and AB–L adhesive layer with lower regions represented by blue-green and higher regions by yellow-red regions, respectively. Inspection of the images bolsters our experiments with carbon black, showing that the IBOA adhesive existed primarily on one side or the other of all of the substrates, pointing toward adhesive failure. In addition, laser profilometry provided a simple means to determine the bond line thickness of our adhesive by measuring the height change from areas of the neat substrate to those where the adhesive resided. After six measurements, we found that the bond line thickness was reasonably constant between 20 and 50  $\mu$ m regardless of the substrate (Table S1).

### 3.4. Investigating the Effect of the Crosslinking Filler.

In a final set of experiments, we strove to increase the glass-transition temperature of our adhesive by incorporating an inorganic/crosslinkable filler in hopes of enhancing the operating temperature. The incorporation of inorganic nanomaterials into adhesives, e.g., polyhedral oligomeric silsesquioxane (POSS), has been shown to improve thermal/mechanical

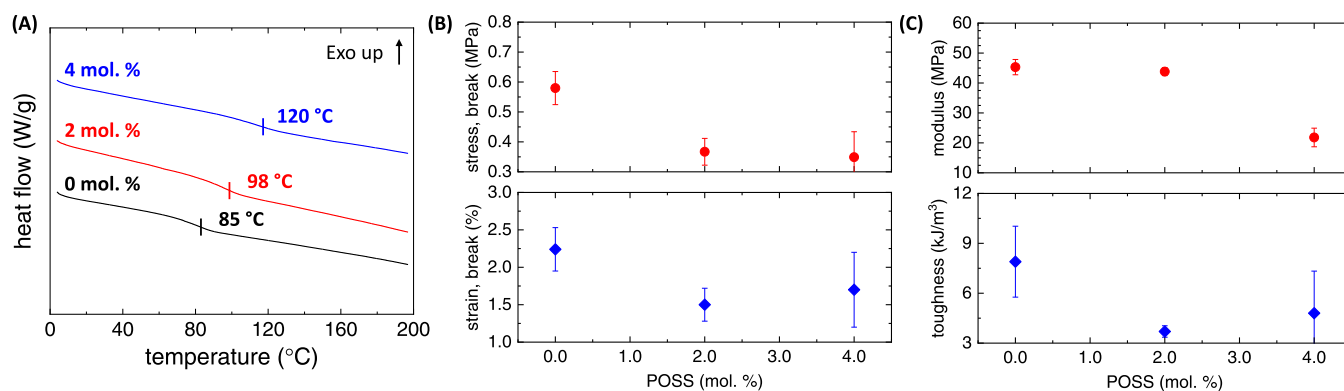


**Figure 6.** Impact of the POSS filler on the thermal properties of pIBOA and adhesive performance. (A) DSC thermograms of the pIBOA adhesive formulated with 0, 2, and 4 mol % POSS from the second heating. (B–C) Impact of POSS on adhesive performance using PP substrates. Adhesive system: bulk IBOA, [AB–L]  $\approx$  1 wt %. [NCO]/[AB–L]  $\approx$  1.25/1, weight press time = 1 h, and cure time = 24 h.

properties and offer a convenient means to tailor properties even at low loadings.<sup>44–47</sup> Inspired by these studies, we employed an eight-arm acrylate-functionalized POSS at low loadings because it could readily undergo copolymerization/crosslinking with our adhesive. Indeed, after incorporation of POSS, the glass-transition temperature increased, changing from 85 to 98 °C using 2 mol % POSS and further to 120 °C with 4 mol % (Figure 6A). This 35 °C enhancement in the  $T_g$  can be attributed to the hindered mobility of pIBOA chains after crosslinking.<sup>48</sup> Motivated by the improvement in  $T_g$ , we subsequently explored the impact of POSS on the adhesive performance. Overall, our lap-shear experiments revealed that higher concentrations of POSS resulted in a decreased mechanical performance as evidenced by a reduced modulus and stress at break from 0.58 to 0.35 MPa and 43–22 MPa, respectively (Figure 6B,C). Strain at break and toughness values were statistically inconclusive but appeared to exhibit a slight decline in performance when using 4 mol % POSS. Hence, this experimentation revealed that a trade-off exists between boosting the thermal properties at the expense of adhesive performance via POSS.

In summary, we have developed an acrylate-based adhesive capable of bonding polymeric substrates rapidly under ambient conditions using complexed alkylboranes. Through optimization experiments, an acrylic monomer and isocyanate deblocker were found to provide the highest monomer conversion with the least amount of the initiator, whereas kinetic studies confirmed that a rapid polymerization occurred in minutes with IBOA and IPDI. After developing a high-yield adhesive formulation, lap-shear experiments were used to evaluate the adhesive's performance, revealing strong adhesion of PP substrates in 20 min and that an intermediate concentration of AB–L provided the best adhesive performance. The effectiveness of the AB–L adhesion platform was found to be generic, successfully bonding a wide range of seven commodity polymer substrates. To increase the operation temperature of the AB–L adhesive, a crosslinkable POSS filler was investigated, which was able to enhance the  $T_g$  of the adhesive but at the expense of the adhesive performance. In this contribution, we reported and investigated a unique acrylate-based adhesive that is driven by an alkylborane initiator complex, which is capable of adhering a wide range of polymeric substrates under exceedingly simple conditions without elevated temperatures, vacuum, or extensive surface treatments. We strive to further improve the adhesive

performance of the AB–L adhesive platform and believe that it holds promise for enabling rapid manufacturing and a potential adhesive for the automotive, aerospace, and marine sectors.

## ■ ASSOCIATED CONTENT

### Supporting Information

The Supporting Information is available free of charge at <https://pubs.acs.org/doi/10.1021/acsomega.2c03740>.

Acrylate (IBOA), methacrylate (IBOMA), and styrene monomer conversion; stress–strain curves for alkylborane concentration, cure times, and control experiments without surface preparation; strain at break for all polymeric substrates; impact of the carbon black filler on stress at break; individual stress–strain curves for all seven polymeric substrates; stress–strain curves for POSS formulations; table of bond line thickness with a laser profilometer (PDF)

## ■ AUTHOR INFORMATION

### Corresponding Author

Andrew J. D. Magenau – Department of Materials Science and Engineering, Drexel University, Philadelphia, Pennsylvania 19104, United States; [orcid.org/0000-0002-7565-9075](https://orcid.org/0000-0002-7565-9075); Email: [ajm496@drexel.edu](mailto:ajm496@drexel.edu)

### Authors

Olivia R. Wilson – Department of Materials Science and Engineering, Drexel University, Philadelphia, Pennsylvania 19104, United States

Dominick J. Borrelli – Department of Materials Science and Engineering, Drexel University, Philadelphia, Pennsylvania 19104, United States

Complete contact information is available at: <https://pubs.acs.org/10.1021/acsomega.2c03740>

### Notes

The authors declare no competing financial interest.

## ■ ACKNOWLEDGMENTS

A.J.D.M. and O.R.W. are grateful to the Graduate Assistance in Areas of the National Need (GAANN P200A180026) Program in the U.S. Department of Education, the ACS Petroleum Research Fund (59903-DNI7), and the Pennsylvania Department of Community & Economic Development

(PA Manufacturing Innovation Program) for partial support for this research. A.J.D.M. and O.R.W. also thank Dr. Yury Gogotsi and Mark Anayee for use of a Keyence Profilometer, Dr. Nicolas Alvarez and Dr. Giuseppe Palmese for use of an Instron tensile tester, and Dr. Christopher Li for use of DSC. MarvinSketch is also gratefully acknowledged for its generous allowance of an academic license for NMR simulations. O.R.W. and D.J.B. are also grateful to the Drexel Machine Shop for their assistance with cutting substrates to specified dimensions and for manufacturing the lap-shear assembly jig.

## REFERENCES

- (1) Bogue, R. Recent innovations in adhesive technology. *Assem. Autom.* **2015**, *35*, 201–205.
- (2) Awaja, F.; Gilbert, M.; Kelly, G.; Fox, B.; Pigram, P. J. Adhesion of polymers. *Prog. Polym. Sci.* **2009**, *34*, 948–968.
- (3) Brewis, D. M.; Briggs, D. Adhesion to polyethylene and polypropylene. *Polymer* **1981**, *22*, 7–16.
- (4) Kinloch, A. J. Toughening epoxy adhesives to meet today's challenges. *MRS Bull.* **2003**, *28*, 445–448.
- (5) Rudawska, A.; Czarnota, M. Selected aspects of epoxy adhesive compositions curing process. *J. Adhes. Sci. Technol.* **2013**, *27*, 1933–1950.
- (6) Rudawska, A. The influence of curing conditions on the strength of adhesive joints. *J. Adhes.* **2020**, *96*, 402–422.
- (7) Pizzi, A.; Mittal, K. L., *Handbook of Adhesive Technology*; 3rd ed.; CRC Press, 2017.
- (8) Wilson, O. R.; McDaniel, R. M.; Rivera, A. D.; Magenau, A. J. D. Alkylborane-Initiated Thiol-Ene Networks for the Synthesis of Thick and Highly Loaded Nanocomposites. *ACS Appl. Mater. Interfaces* **2020**, *12*, 55262–55268.
- (9) Wilson, O. R.; Magenau, A. J. D. Oxygen Tolerant and Room Temperature RAFT through Alkylborane Initiation. *ACS Macro Lett.* **2018**, *7*, 370–375.
- (10) Timmins, R. L.; Wilson, O. R.; Magenau, A. J. D. Arm-first star-polymer synthesis in one-pot via alkylborane-initiated RAFT. *J. Polym. Sci.* **2020**, *58*, 1463–1471.
- (11) Tran-Do, M.-L.; Habas, J.-P.; Ameduri, B. Oxygen-Tolerant Alternating Copolymerization of Fluorinated Monomers and Vinyl Ethers at Mild Temperature. *ACS Appl. Polym. Mater.* **2022**, *4*, 1401–1410.
- (12) Peng, Y.; Liu, S.; Wang, L.; Xu, Y.; Wu, Z.; Chen, H. Oxygen-Demanding Photocontrolled RAFT Polymerization Under Ambient Conditions. *Macromol. Rapid Commun.* **2022**, *43*, No. 2100920.
- (13) Lv, C.; Du, Y.; Pan, X. Alkylboranes in Conventional and Controlled Radical Polymerization. *J. Polym. Sci.* **2020**, *58*, 14–19.
- (14) Corrigan, N.; Jung, K.; Boyer, C. Merging New Organoborane Chemistry with Living Radical Polymerization. *Chem* **2020**, *6*, 1212–1214.
- (15) Sonnenschein, M. F.; Webb, S. P.; Rondan, N. Amine Organoborane Complex Polymerization Initiators and Polymerizable Compositions. U.S. Patent US6,706,8312004.
- (16) Skoultchi, M. M.; Merlo, N. V. Acrylic adhesive composition and organoboron initiator system. U.S. Patent US5,106,9281992.
- (17) Zharov, J. V.; Krasno, J. N. Polymerizable compositions made with polymerization initiator systems based on organoborane amine complexes. U.S. Patent US5,539,0701996.
- (18) Maandi, E. Bonding system having adherence to low energy surfaces. U.S. Patent US6,632,9082003.
- (19) Kendall, J. L.; Righettini, R. F.; Abbey, K. J. Internally blocked organoborane initiators and adhesives therefrom. U.S. Patent US6,646,0762004.
- (20) Diakoumakos, C. D.; Kotzev, D. L. Initiator systems for polymerisable compositions. WO2005/044867A12005.
- (21) Dodonov, V. A.; Starostina, T. I. Radical Bonding Thermoplastics and Materials with Low Surface Energy Using Acrylate Compositions. *Polym. Sci., Ser. D* **2018**, *11*, 60–66.
- (22) Sonnenschein, M. F.; Webb, S. P.; Redwine, O. D.; Wendt, B. L.; Rondan, N. G. Physical and Chemical Probes of the Bond Strength between Trialkylboranes and Amines and Their Utility as Stabilized Free Radical Polymerization Catalysts. *Macromolecules* **2006**, *39*, 2507–2513.
- (23) Li, M.; Zheng, Z.; Liu, S.; Wei, W.; Wang, X. Effect of prepolyurethane on the performances of poly(acrylates-co-urethane) copolymer. *J. Appl. Polym. Sci.* **2010**, *118*, 3203–3210.
- (24) Brown, H. C.; Midland, M. M. Initiation rates for autoxidation of trialkylboranes. Effect of a steric factor on the initiation rate. *J. Chem. Soc. D* **1971**, 699–700.
- (25) Sonnenschein, M. F.; Webb, S. P.; Kastl, P. E.; Arriola, D. J.; Wendt, B. L.; Harrington, D. R.; Rondan, N. G. Mechanism of Trialkylborane Promoted Adhesion to Low Surface Energy Plastics. *Macromolecules* **2004**, *37*, 7974–7978.
- (26) Ligon, S. C.; Husár, B.; Wutzel, H.; Holman, R.; Liska, R. Strategies to Reduce Oxygen Inhibition in Photoinduced Polymerization. *Chem. Rev.* **2014**, *114*, 557–589.
- (27) Lv, C.; He, C.; Pan, X. Oxygen-Initiated and Regulated Controlled Radical Polymerization under Ambient Conditions. *Angew. Chem., Int. Ed.* **2018**, *57*, 9430–9433.
- (28) Okamura, H.; Sudo, A.; Endo, T. Generation of radical species on polypropylene by alkylborane-oxygen system and its application to graft polymerization. *J. Polym. Sci., Part A: Polym. Chem.* **2009**, *47*, 6163–6167.
- (29) Garrett, G. E.; Pratt, D. A.; Parent, J. S. Hydrogen Atom Abstraction from Polyolefins: Experimental and Computational Studies of Model Systems. *Macromolecules* **2020**, *53*, 2793–2800.
- (30) Standard Test Method for Determining Strength of Adhesively Bonded Rigid Plastic Lap-Shear Joints in Shear by Tension Loading. *ASTM* **2014**, 1–3.
- (31) Brandrup, J.; Immergut, E.H.; Grulke, E.A. *Polymer Handbook*, 4th ed.; Wiley: New York, 1999.
- (32) Beuermann, S.; Buback, M. Rate coefficients of free-radical polymerization deduced from pulsed laser experiments. *Prog. Polym. Sci.* **2002**, *27*, 191–254.
- (33) Ahn, D.; Wier, K. A.; Mitchell, T. P.; Olney, P. A. Applications of Fast, Facile, Radiation-Free Radical Polymerization Techniques Enabled by Room Temperature Alkylborane Chemistry. *ACS Appl. Mater. Interfaces* **2015**, *7*, 23902–23911.
- (34) Raos, G.; Zappone, B. Polymer Adhesion: Seeking New Solutions for an Old Problem. *Macromolecules* **2021**, *54*, 10617–10644.
- (35) Williamson, J. B.; Lewis, S. E.; Johnson, R. R., III; Manning, I. M.; Leibfarth, F. A. C–H Functionalization of Commodity Polymers. *Angew. Chem., Int. Ed.* **2019**, *58*, 8654–8668.
- (36) Cole, P. J.; Cook, R. F.; Macosko, C. W. Adhesion between Immiscible Polymers Correlated with Interfacial Entanglements. *Macromolecules* **2003**, *36*, 2808–2815.
- (37) Luo, Y.-R. *Comprehensive Handbook of Chemical Bond Energies*, CRC Press, 2007.
- (38) McGinty, K. M.; Brittain, W. J. Hydrophilic surface modification of poly(vinyl chloride) film and tubing using physisorbed free radical grafting technique. *Polymer* **2008**, *49*, 4350–4357.
- (39) Blanksby, S. J.; Ellison, G. B. Bond Dissociation Energies of Organic Molecules. *Acc. Chem. Res.* **2003**, *36*, 255–263.
- (40) Bukowski, C.; Zhang, T.; Riggelman, R. A.; Crosby, A. J. Load-bearing entanglements in polymer glasses. *Sci. Adv.* **2021**, *7*, No. eabg9763.
- (41) Bowden, P. B. The elastic modulus of an amorphous glassy polymer. *Polymer* **1968**, *9*, 449–454.
- (42) Haward, R. N.; MacCallum, J. R. The relationship between volume and elasticity in polymer glasses. *Polymer* **1971**, *12*, 189–194.
- (43) Jakubowski, W.; Juhari, A.; Best, A.; Koynov, K.; Pakula, T.; Matyjaszewski, K. Comparison of thermomechanical properties of statistical, gradient and block copolymers of isobornyl acrylate and n-butyl acrylate with various acrylate homopolymers. *Polymer* **2008**, *49*, 1567–1578.

- (44) Kuo, S.-W. Hydrogen bonding interactions in polymer/polyhedral oligomeric silsesquioxane nanomaterials. *J. Polym. Res.* **2022**, *29*, No. 69.
- (45) Dodiuk, H.; Kenig, S.; Blinsky, I.; Dotan, A.; Buchman, A. Nanotailoring of epoxy adhesives by polyhedral-oligomeric-silsesquioxanes (POSS). *Int. J. Adhes. Adhes.* **2005**, *25*, 211–218.
- (46) Hanifpour, A.; Bahri-Laleh, N.; Nekoomanesh-Haghighi, M. Methacrylate-functionalized POSS as an efficient adhesion promoter in olefin-based adhesives. *Polym. Eng. Sci.* **2020**, *60*, 2991–3000.
- (47) Mirmohammadi, S. A.; Nekoomanesh-Haghighi, M.; Mohammadian Gezaz, S.; Bahri-Laleh, N.; Atai, M. In-situ photocrosslinkable nanohybrid elastomer based on polybutadiene/polyhedral oligomeric silsesquioxane. *Mater. Sci. Eng. C* **2016**, *68*, 530–539.
- (48) Xu, H.; Yang, B.; Wang, J.; Guang, S.; Li, C. Preparation, Tg improvement, and thermal stability enhancement mechanism of soluble poly(methyl methacrylate) nanocomposites by incorporating octavinyl polyhedral oligomeric silsesquioxanes. *J. Polym. Sci., Part A: Polym. Chem.* **2007**, *45*, 5308–5317.